Interaction of Ba^{2+} with the Pores of the Cloned Inward Rectifier K^+ Channels Kir2.1 Expressed in *Xenopus* Oocytes

Ru-Chi Shieh,* Jui-Chu Chang,* and Jorge Arreola#

*Institute of Biomedical Sciences, Academia Sinica, Taipei 11529, Taiwan, R.O.C., and #Instituto de Física, Universidad Autónoma de San Luis Potosí, San Luis Potosí, S.L.P. 78000, Mexico

ABSTRACT Interactions of Ba^{2+} with K^+ and molecules contributing to inward rectification were studied in the cloned inward rectifier K^+ channels, Kir2.1. Extracellular Ba^{2+} blocked Kir2.1 channels with first-order kinetics in a V_m-dependent manner. At V_m more negative than −120 mV, the K_d-V_m relationship became less steep and the dissociation rate constants were larger, suggesting Ba^{2+} dissociation into the extracellular space. Both depolarization and increasing $[K^+]_i$ accelerated the recovery from extracellular Ba^{2+} blockade. Intracellular K^+ appears to relieve Ba^{2+} blockade by competitively slowing the Ba^{2+} entrance rate, instead of increasing its exit rate by knocking off action. Intracellular spermine (100 μM) reduced, whereas 1 mM $[Mg^{2+}]_i$ only slightly reduced, the ability of intracellular K^+ to repulse Ba^{2+} from the channel pore. Intracellular Ba^{2+} also blocked outward $I_{Kir2.1}$ in a voltage-dependent fashion. At $V_m \geq +40$ mV, where intrinsic inactivation is prominent, intracellular Ba^{2+} accelerated the inactivation rate of the outward $I_{Kir2.1}$ in a V_m-independent manner, suggesting interaction of Ba^{2+} with the intrinsic gate of Kir2.1 channels.

INTRODUCTION

Inward rectifier K^+ channels conduct inward currents at potentials more negative than the K^+ reversal potential but permit much smaller currents at potentials positive to the reversal potential (Hille, 1992). Thus inward rectifier K^+ channels set the resting membrane potential and control the excitability of many cell types. Two mechanisms have been proposed to account for inward rectification of K^+ channels. The first involves the voltage-dependent blockade of outward K^+ currents by both intracellular Mg^{2+} (Matsuda et al., 1987; Vandenberg, 1987) and polyamines (Fickler et al., 1994; Lopatin et al., 1994). These observations are consistent with the hypothesis that inward rectification is caused by intracellular pore blocking particle(s) (Hille and Schwarz, 1978). The second mechanism is a novel pH_i-dependent gating mechanism that is involved in the inactivation of the outward currents and is independent of intracellular Mg^{2+} and polyamines (Shieh et al., 1996).

Ba^{2+} is known to inhibit several types of K^+ channels expressed in different tissues, including delayed rectifier K^+ channels of squid giant axon (Armstrong and Taylor, 1980; Eaton and Brodwick, 1980; Armstrong et al., 1982), native inward rectifier K^+ channels of starfish eggs and frog skeletal muscle (Hagiwara et al., 1978; Standen and Stanfield, 1978), and Ca^{2+}-activated K^+ channels (Vergara and Latorre, 1983; Neyton and Miller, 1988a,b). The inhibitory effects of extracellular Ba^{2+} have also been demonstrated in different cloned inward rectifier K^+ channels, including those cloned from mouse macrophage (Kubo et al., 1993), human and mouse brain (Makhina et al., 1994; Morishige et al., 1994; Perier et al., 1994), rat kidney (Zhou et al., 1996), and human heart (Ashen et al., 1995). Application of extracellular Ba^{2+} to either native or cloned inward rectifier K^+ channels resulted in voltage- and time-dependent inhibitions of the K^+ currents. In contrast, the application of extracellular Ba^{2+} to the delayed rectifier K^+ channels from squid axon reduced the magnitude of K^+ current without changing its kinetics, whereas intracellular Ba^{2+} induced time-dependent inhibition of the channels (Armstrong and Taylor, 1980; Eaton and Brodwick, 1980; Armstrong et al., 1982). However, detailed characterization of Ba^{2+} blockade in the cloned inward rectifier K^+ channels has not been carried out.

Because Ba^{2+} and K^+ have similar crystal radii, it has been hypothesized that Ba^{2+} ions inhibit K^+ channels by entering the pores when the channels are opened by changes in membrane potential, as evidenced by the findings that extracellular K^+ could either knock off the Ba^{2+} (Eaton and Brodwick, 1980; Armstrong and Taylor, 1980) or compete for the Ba^{2+} binding site (Vergara and Latorre, 1983) in K^+ channels. These previous studies suggest that the voltage-dependent inhibition of K^+ channels by Ba^{2+} is due to the interaction of Ba^{2+} ions with the amino acid residues lining the pores of the channels, which are presumably located within the electrical field. Thus Ba^{2+} has been used as a probe to learn about the permeability of the K^+ channels. For example, from the studies of K^+ and Ba^{2+} interaction in the pores of the high-conductance Ca^{2+}-activated K^+ channels, it has been shown that each channel has at least three binding sites for the permeant K^+ ions (Neyton and Miller, 1988b).

In this study we examined the interactions of Ba^{2+} with the permeant K^+ ion in Kir2.1 channels and found that extracellular Ba^{2+} blockade was relieved by intracellular K^+ through competition for the same binding site. Ba^{2+}

Received for publication 21 January 1998 and in final form 28 July 1998.

Address reprint requests to Dr. Ru-Chi Shieh, Institute of Biomedical Sciences, Academia Sinica, 128 Yen-Chiu Yuan Road, Section 2, Taipei 11529, Taiwan, R.O.C. Tel.: 02-2789-9024; Fax: 02-2785-3569; E-mail: ruchi@novell.ibms.sinica.edu.tw.

0006-3495/98/11/2313/10 $2.00

thus is a useful probe for studying K^+ binding in Kir2.1 channels. In addition, we identified the interactions of Ba^{2+} with the rectifying factors, including intracellular Mg^{2+} and spermine and the "intrinsic" gate. The results demonstrate that although both Mg^{2+} and spermine induce inward rectification by blocking the Kir2.1 channel, their binding sites are not identical. Ba^{2+} applied intracellularly appears to accelerate the inactivation of outward current by interfering with the "intrinsic" gating mechanism and thus is a potential tool for unraveling the essence of the intrinsic gating property of the Kir2.1 channel. A preliminary report of these findings has been presented to the Biophysical Society (Shieh et al., 1998).

MATERIALS AND METHODS

Molecular biology and preparation of *Xenopus* oocytes

Mouse macrophage Kir2.1 DNA (the original clone in pCDNPAI/Amp was generously provided by Dr. Lily Jan, UCSF)) subcloned into Bluescript II SK+ was a generous gift from Drs. Scott A. John and James N. Weiss (UCLA). Purified linear Kir2.1 DNA and in vitro transcription were carried out as previously described (Shieh et al., 1996).

Xenopus oocytes were obtained by partial ovariectomy from frogs fully anesthetized with 0.1% tricaine and then defolliculated using 2% collagenase as previously described (Shieh et al., 1996). Oocytes were pressure injected 24 h after defolliculation with 10–100 pg of Kir2.1 cRNAs for whole-cell recordings and 1–10 ng for giant patch recordings. Oocytes were maintained at 18°C in Barth's solution containing (in mM) 88 NaCl, 1 KCl, 2.4 $NaHCO_3$, 0.3 $Ca(NO_3)_2$, 0.41 $CaCl_2$, 0.82 $MgSO_4$, 15 HEPES, and 20 μg gentamicin/ml at pH 7.6 and were used 1–3 days after RNA injection.

Electrophysiology techniques

Extracellular Ba^{2+} blockade of whole-cell $I_{Kir2.1}$ was examined at room temperature (21–24°C) using a two-electrode voltage-clamp amplifier (Ca-1 clamp; Dagan, Minneapolis, MN). Oocytes were bathed in a solution containing (in mM) 98 KCl, 2 KOH, 1.8 $CaCl_2$, and 5 HEPES at pH 7.4. Both the voltage-sensing and current-injecting electrodes were filled with 3 M KCl (resistance 0.2–1 MΩ). Voltage steps were applied from a holding potential of 0 mV to various test voltages ranging from -160 to $+40$ mV in 10-mV increments. To ensure that Ba^{2+} blockade reached steady state, the effects of $[Ba^{2+}] \leq 30$ μM were studied using 10-s depolarizing pulses, whereas those of $[Ba^{2+}] \geq 100$ μM were examined using 2-s pulses. Ba^{2+} was added directly to the bath solution until the desired concentration was reached, and the pH was adjusted to 7.4.

To avoid inadequate voltage clamping in whole cells caused by large currents, we used oocytes expressing an absolute value of less than -10 μA at -160 mV. The time constants for the blockade (τ_{block}) of the $I_{Kir2.1}$ recorded at -120 mV by 10 μM $[Ba^{2+}]$ in whole cells (123.6 $\pm$ 8.8 ms, $n = 13$) were not significantly different ($p = 0.19$) from those recorded in cell-attached patches (104.3 $\pm$ 10.4 ms, $n = 8$). Furthermore, the recovery time constants in cell-attached patches (τ_{recov} = 412.3 $\pm$ 33.6 ms, $n = 8$) were not significantly different ($p = 0.49$) from those obtained in whole cells (τ_{recov} = 385.9 $\pm$ 9.8 ms, $n = 7$) at $V_r = +100$ mV. These data suggest that the voltage clamping in whole cells was as adequate as that in patches.

In experiments where intracellular ionic conditions needed to be changed, $I_{Kir2.1}$ was recorded using the inside-out giant patch-clamp technique (Hilgemann, 1995; Shieh et al., 1996) and an Axopatch 1-D amplifier (Axon Instruments, Foster City, CA). Patch electrode solution contained (in mM) 98 KCl, 2 KOH, 1.8 $CaCl_2$ (or 5 $MgCl_2$), and 5 HEPES at pH 7.4. Bath solution (control intracellular solution) contained (in mM) 82 KCl, 18 KOH, 5 EDTA, 2 K_2ATP, and 5 HEPES at pH 7.2. Concentrations of K^+ from 200 mM down to 20 mM were obtained by changing the concentrations of KCl while the concentrations of HEPES, EDTA, and KOH were kept constant. The rundown of channel activity was avoided by treating the patches with 25 μM L-α- phosphatidylinositol-4,5-bisphosphate (PIP_2) (Sigma Chemical Co., St. Louis, MO) (Huang et al., 1998) for 20–60 s. PIP_2 stock solution (1 mM) was prepared by dissolving PIP_2 in chloroform. On the day of experiments, 125 μl of the stock solution was N_2-dried and resuspended in 5 ml of control intracellular solution by sonication for 15 s three times, separated by 30-s intervals. Although the amplitude of outward $I_{Kir2.1}$ was increased by 25 μM PIP_2, the recovery from the extracellular Ba^{2+} blockade and the intrinsic inactivation of the outward currents were not significantly different ($p > 0.1$) between patches treated with and without PIP_2 (data not shown). To wash out the residual intracellular Mg^{2+} and polyamines, experiments were carried out after at least 5 min of continuous perfusion of Mg^{2+}- and polyamine-free solution after patch excision. Free $[Ba^{2+}]$ and $[Mg^{2+}]$ in the intracellular solution were calculated with the MaxC program (Chris Patton, Stanford University) and stability constants by Martell and Smith (1974).

The command voltage pulses and data acquisition functions were processed using a Pentium 100 computer, a DigiData board, and pClamp6 software (Axon Instruments, Burlingame, CA). Data were filtered at 1 kHz by a 8-pole low-pass filter (Frequency Devices, Rochester, NY). Frequencies of stimulation and data sampling are described in the figure legends.

Data analysis

Students' independent or paired *t*-test was used to assess statistical significance. Results are presented as mean $\pm$ SEM.

RESULTS

The blockade of inward $I_{Kir2.1}$ by extracellular Ba^{2+}

Fig. 1 *A* shows current traces recorded at -120 mV from a representative oocyte in the absence and in the presence of the indicated $[Ba^{2+}]_o$. The addition of Ba^{2+} to the extracellular side of the membrane induced a time-dependent decrease of the inward currents. The rate of inhibition of $I_{Kir2.1}$ was accelerated by increasing $[Ba^{2+}]_o$, and the currents reached steady state at the end of hyperpolarization. $I_{Kir2.1}$ at the onset of hyperpolarization was little affected by Ba^{2+}. For example, 10 μM $[Ba^{2+}]_o$ reduced the instantaneous $I_{Kir2.1}$ recorded at -120 mV by only 5 $\pm$ 2% ($n = 6$), despite the fact that at the end of the pulse less than 5% of the current remained. This observation suggests that the Kir2.1 channels are not affected by Ba^{2+} at 0 mV, and channels must open before Ba^{2+} inhibition takes place.

Normalized steady state current-voltage (*I-V*) relationships in the presence of various $[Ba^{2+}]_o$ are summarized in Fig. 1 *B*, which shows that the effects of extracellular Ba^{2+} on $I_{Kir2.1}$ were voltage dependent. Extracellular Ba^{2+} preferentially affected Kir2.1 channels at more negative potentials. This voltage-dependent effect of $[Ba^{2+}]_o$ (1 or 10 μM) on Kir2.1 channels resulted in a negative conductance at negative potentials (Fig. 1 *B*), as has previously been observed in Kir2.1 channels (Kubo et al., 1993).

Fig. 1 *C* shows, from left to right, the dose-response curves for the blockade of the steady-state $I_{Kir2.1}$ by extra-

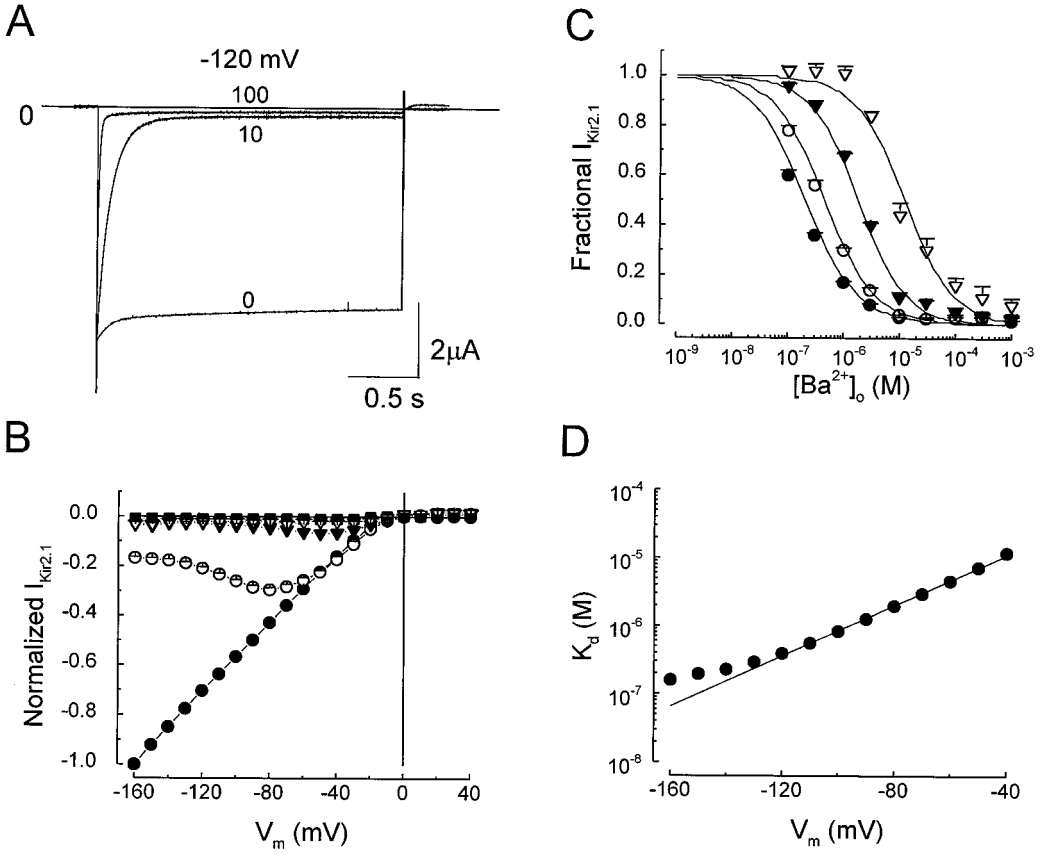

FIGURE 1 Blockade of inward $I_{Kir2.1}$ by extracellular Ba^{2+}. (*A*) Representative currents elicited by voltage steps to −120 mV for 2 s from a holding potential of 0 mV in the presence of the indicated $[Ba^{2+}]_o$ (μM). The horizontal line indicates the zero current level. Current traces recorded in the presence of 5 mM $[Ba^{2+}]_o$ were used to eliminate the linear leak currents. (*B*) Normalized current-voltage (*I-V*) relationships for the steady-state inward $I_{Kir2.1}$. Data are the averages from 4–12 cells in the presence of 0 (●), 1 (○), 10 (▼), 100 (▽), and 1000 μM Ba^{2+} (■). Steady-state currents measured at the end of the 2- or 10-s pulses were normalized to that recorded at −160 mV in the absence of Ba^{2+} in each cell and then averaged. (*C*) Dose-response curves for extracellular Ba^{2+} blockade of the steady-state $I_{Kir2.1}$ at −160 mV (●), −120 mV (○), −80 mV (▼), and −40 mV (▽). Lines are the best fits to the averaged data (n = 4–12 for each point) using the Hill equation (Eq. 1). (*D*) K_d values obtained from the concentration-dependent inhibition of the steady-state $I_{Kir2.1}$ are plotted against membrane potentials. The solid line is the best fit of the data obtained at V_m ranging from −120 mV to −40 mV, using the Boltzmann equation (Eq. 2). The frequencies of stimulation were 0.05–0.083 Hz, and the sampling rates of the $I_{Kir2.1}$ were 1.43–1.67 kHz.

cellular Ba^{2+} at V_m = −160, −120, −80, and −40 mV. $I_{Kir2.1}$ amplitude was normalized to the control amplitude ($[Ba^{2+}]_o$ = 0) obtained at the same potential and expressed as fractional $I_{Kir2.1}$. The dose-response curves also demonstrate the voltage-dependent inhibition of the inward $I_{Kir2.1}$ by extracellular Ba^{2+}. As the membrane potential became more hyperpolarized, the steady-state $I_{Kir2.1}$ was more sensitive to extracellular Ba^{2+}, as if the negative electrical field attracted Ba^{2+} inside the membrane. The dose-response curves at each potential were well described by the Hill equation (Eq. 1):

$$\text{Fractional } I_{Kir2.1} = \frac{1}{1 + \left(\frac{[Ba^{2+}]}{K_d}\right)^n} \quad (1)$$

where K_d is the apparent dissociation constant and n is the Hill coefficient. The K_d values obtained from the fittings were 0.2 μM, V_m = −160 mV; 0.5 μM, V_m = −120 mV; 2.2 μM, V_m = −80 mV; 12.7 μM, V_m = −40 mV. The Hill coefficients were 0.84, V_m = −160 mV; 0.90, V_m = −120 mV; 1.06, V_m = −80 mV; 0.99, V_m = −40 mV. The corresponding Hill coefficients were close to 1, suggesting one Ba^{2+} interacted with one channel protein.

To quantitatively assay the voltage dependence of the inhibition of $I_{Kir2.1}$ by extracellular Ba^{2+}, the K_d values obtained from the blockade of the steady-state $I_{Kir2.1}$ were plotted against the membrane potential (Fig. 1 *D*). The solid line is the fit to the data points from −40 to −120 mV, using the Boltzmann equation:

$$K_d = K_d(0) \cdot \exp\left[\frac{z\delta F}{RT}(V_m)\right] \quad (2)$$

where $K_d(0)$ is the dissociation constant at 0 mV, z is the valence of Ba^{2+} = +2, δ is the apparent electrical distance between the Ba^{2+}-channel interacting site and the outer pore of the channel, and F, R, T, and V_m have their usual meanings. The estimated $K_d(0)$ was 62 μM, and δ was 0.54 for the blockade of steady-state $I_{Kir2.1}$. Note that the K_d-V_m

relationship became less steep at V_m more negative than −120 mV. This may be due to Ba^{2+} dissociation into the intracellular site at very negative V_m, as previously described in the high-conductance Ca^{2+}-activated K^+ channel (Neyton and Miller, 1988b).

Kinetics of the extracellular Ba^{2+}-induced blockade of Kir2.1 channels

To quantitatively examine the kinetics of the blockade of Kir2.1 channels by extracellular Ba^{2+}, we obtained the association (k_{on}) and dissociation (k_{off}) rate constants of Ba^{2+} interacting with the binding site. Assuming the interaction of Ba^{2+} with Kir2.1 channels follows a first-order reaction, as suggested by the dose-response curves (Fig. 1 *C*), we can then compute k_{on} and k_{off}, using the equations described by Holmgren et al. (1997):

$$k_{on} = \frac{1 - f}{\tau_{block} \times [Ba^{2+}]} \quad (3)$$

$$k_{off} = \frac{f}{\tau_{block}} \quad (4)$$

where $f = I_{steady\text{-}state}/I_{ctrl}$.

Fig. 2 *A* summarizes the k_{on}-V_m relationship. The solid line is the fit to the data points from −40 to −120 mV, using the Boltzmann equation with a k_{on} at 0 mV = 6.8×10^3 $s^{-1}M^{-1}$ and a $\delta = 0.52$. This value of δ was comparable to that (0.54) obtained using stationary analysis of dose-response curves (Fig. 1 *C*). These results demonstrate that the voltage-dependent interaction of Ba^{2+} ions with the binding sites in the channels to induce blockade of Kir2.1 channels is mainly due to the voltage dependence of k_{on}. In contrast, the k_{off}-V_m relationship (Fig. 2 *B*) showed little V_m dependence at V_m between −130 and −50 mV. However, k_{off} increased as V_m became more negative than −130 mV. These results are indicative of Ba^{2+} dissociating into the intracellular space, as previously shown in the high-conductance Ca^{2+}-activated K^+ channels (Neyton and Miller, 1988b) and Shaker K^+ channels (Harris et al., 1998). This is also consistent with the observation that the K_d-V_m relationship became less steep at V_m more negative than −120 mV.

Recovery of Kir2.1 channels from extracellular Ba^{2+} blockade

Fig. 2 *B* shows that k_{off} tends to increase at $V_m > -50$ mV. Unfortunately, currents recorded at $V_m > -40$ mV were too small to allow us to estimate k_{off} at more positive V_m. To obtain experimental estimates of k_{off} over the positive range of potentials, the rate of recovery from 10 μM $[Ba^{2+}]_o$ blockade was examined using a two-pulse protocol. The fraction of channels blocked by 10 μM $[Ba^{2+}]_o$ at −120 mV was tested by the first pulse, whereas the fraction of channels recovered from blockade after a given time interval at various recovery voltages (V_r) was recorded by the second pulse. Fig. 3, *A* and *B*, shows the voltage protocol (*A*, *top panel*) with various recovery time intervals and the corresponding current traces recorded with $V_r = 0$ (*A*, *lower panel*) and $V_r = +60$ mV (*B*). $I_{Kir2.1}$ activated by the first hyperpolarizing pulse displayed a monoexponential blockade until only 5% of the instantaneous current amplitude remained at the end of the pulse. The instantaneous current recorded with the second hyperpolarizing pulse increased as the interval between the two pulses increased. The recovery from the blockade followed a monoexponential time course and was faster with $V_r = +60$ mV (time constant = 867 ms) than that with $V_r = 0$ mV (time constant = 1506 ms). The steady-state $I_{Kir2.1}$ at the end of the −120-mV pulse remained constant, independent of the recovery time interval, the recovery voltage, or the fraction of channels recovered at the beginning of the second hyperpolarizing pulse.

The recovery time courses for the instantaneous current recorded at the second pulse at different recovery voltages are shown in Fig. 3 *C*. The fractional recovery was calculated as I_2/I_1, where I_2 was the current recorded 4 ms after

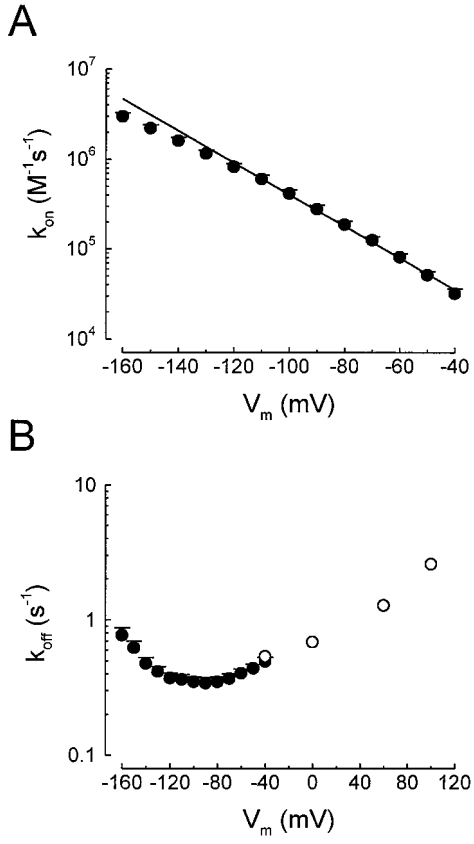

FIGURE 2 Kinetics analysis of inward $I_{Kir2.1}$ blockade by extracellular Ba^{2+}. (*A*) k_{on} values obtained from Eq. 3 are plotted at the corresponding membrane potentials ($n = 6$). The solid line was the fit of the data using the Boltzmann equation. (*B*) The voltage dependence of the k_{off} values computed from Eq. 4 (●, $n = 6$) and those obtained from recovery from extracellular Ba^{2+} blockade experiments (○). k_{on} and k_{off} values were estimated by using f and τ_{block} obtained at $[Ba^{2+}]_o = 3$ μM. Similar k_{on}-V_m and k_{off}-V_m relationships were also observed with $[Ba^{2+}]_o = 1$, 10, and 30 μM.

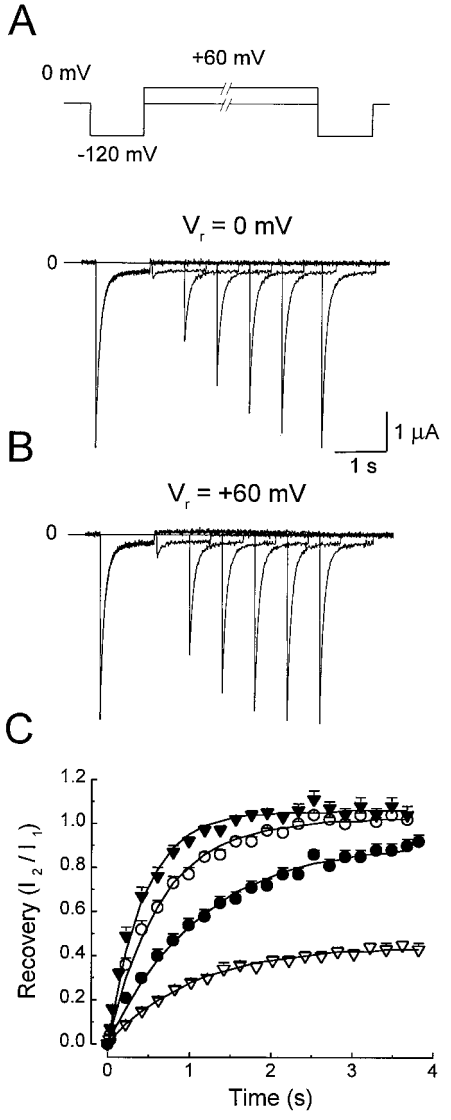

FIGURE 3 Time course of recovery from extracellular Ba^{2+} blockade. (*A*) Upper panel shows the two-pulse voltage protocol. The time interval between the two identical pulses (each for 1 s) was increased by 0.6 s between sweeps (starting at 0.05 s) to assess recovery from blockade induced by extracellular Ba^{2+} (10 μM) during the first pulse. The corresponding current traces recorded with $V_r = 0$ are shown in the lower panel. (*B*) Current traces recorded with $V_r = +60$ mV, using the same protocol as described in *A*. Currents recorded in the presence of 5 mM $[Ba^{2+}]_o$ were subtracted from the currents recorded in 10 μM $[Ba^{2+}]_o$ to eliminate the linear leak currents. The horizontal lines indicate the zero current level. (*C*) Time courses for recovery from extracellular Ba^{2+} blockade with $V_r = -40$ (▽), 0 (●), 60 (○), and 100 (▼) mV. The recovery time constants (τ_{recov}) were 1160 ± 53 ms, $V_r = -40$ mV ($n = 5$); 1315 ± 85 ms, $V_r = 0$ mV ($n = 6$); 775 ± 48 ms, $V_r = +60$ mV ($n = 6$); 386 ± 10 ms, $V_r = +100$ mV ($n = 7$). Continuous lines are single-exponential function fits to the data. The estimated maximum fractional recoveries obtained from fittings were 0.43 ± 0.03, $V_r = -40$ mV ($n = 5$); 0.94 ± 0.03, $V_r = 0$ mV ($n = 6$); 1.01 ± 0.01, $V_r = +60$ mV ($n = 6$); 1.06 ± 0.05, $V_r = +100$ mV ($n = 7$). The frequency of stimulation was 0.04 Hz, and the data sampling rate was 0.5 kHz.

the onset of the second pulse minus the steady-state current, and I_1 was the current recorded 4 ms after the onset of the first pulse minus the steady-state current. The fraction of Kir2.1 channels recovered from extracellular Ba^{2+} blockade followed an exponential time course, as shown by the fits to monoexponential functions. The τ_{recov} values calculated from the monoexponential fits, the k_{on} values described in Fig. 2 *A*, and the function $1/\tau_{recov} = k_{on} \times [Ba^{2+}]_o + k_{off}$ were used to estimate k_{off} at positive voltages. The k_{on} values at 0, +60, and +100 mV were obtained from the extrapolation of the k_{on}-V_m relationship shown in Fig. 2 *A*. The calculated k_{off} values were plotted against V_m in Fig. 2 *B*. k_{off} at −40 mV is very close to k_{off} determined from the kinetic analysis of the extracellular Ba^{2+} blockade. k_{off} obtained from the recovery for the extracellular Ba^{2+} blockade at potentials positive to 0 mV increased significantly ($p < 0.0005$) when compared to that calculated from the kinetic analysis of the extracellular Ba^{2+} blockade at −40 mV. The voltage dependence of k_{off} at positive voltages determined from recovery of blockade is probably due to the effects of the electrical field on the dissociation of Ba^{2+} into the extracellular side.

Effects of intracellular K^+ on the recovery from extracellular Ba^{2+} blockade

To further investigate whether extracellular Ba^{2+} enters the pore of Kir2.1 channels to induce blockade, we examined the effects of intracellular K^+ concentration ($[K^+]_i$) on the recovery from extracellular Ba^{2+} blockade, as previously described for delayed rectifier K^+ channels of squid giant axon (Armstrong and Taylor, 1980). To control the intracellular ionic compositions, $I_{Kir2.1}$ was recorded using a giant patch technique and a voltage protocol similar to that described in Fig. 3 *A*. The hyperpolarizing pulses were set at $V_m = -120$ mV, V_r was set at +100 mV, and the holding potential was set at $V_m = E_K$ throughout this series of experiments. Fig. 4 *A* shows a set of $I_{Kir2.1}$ currents recorded from a cell-attached patch, with a pipette solution containing 10 μM $[Ba^{2+}]$ used to induce blockade. The overall characteristics (τ_{block} and τ_{recov}) of $I_{Kir2.1}$ recorded in cell-attached patches were similar to those recorded in whole cells (compare to Fig. 3). When the same patch was excised (inside out) into a Mg^{2+}-free and polyamine-free control intracellular solution, both the rate of the blockade for the inward $I_{Kir2.1}$ and the rate of the recovery from extracellular Ba^{2+} blockade were increased (Fig. 4 *B*), and outward currents were observed during the recovery interval. τ_{block} decreased from 106 ms to 47 ms, and τ_{recov} decreased from 452 ms to 42 ms. When the same patch was perfused with an intracellular solution containing only 20 mM $[K^+]$, the outward current decreased at $V_r = +100$ mV, τ_{recov} increased from 42 to 62 ms, and τ_{block} decreased from 47 to 22 ms (Fig. 4 *C*).

It was previously considered that there are two possible mechanisms for relief of the channel blocker by intracellular K^+ (Yellen, 1984). One is that K^+ relieves the block by competing with the blocker for the same binding site in the channel. The other is that K^+ accelerates the exit of the

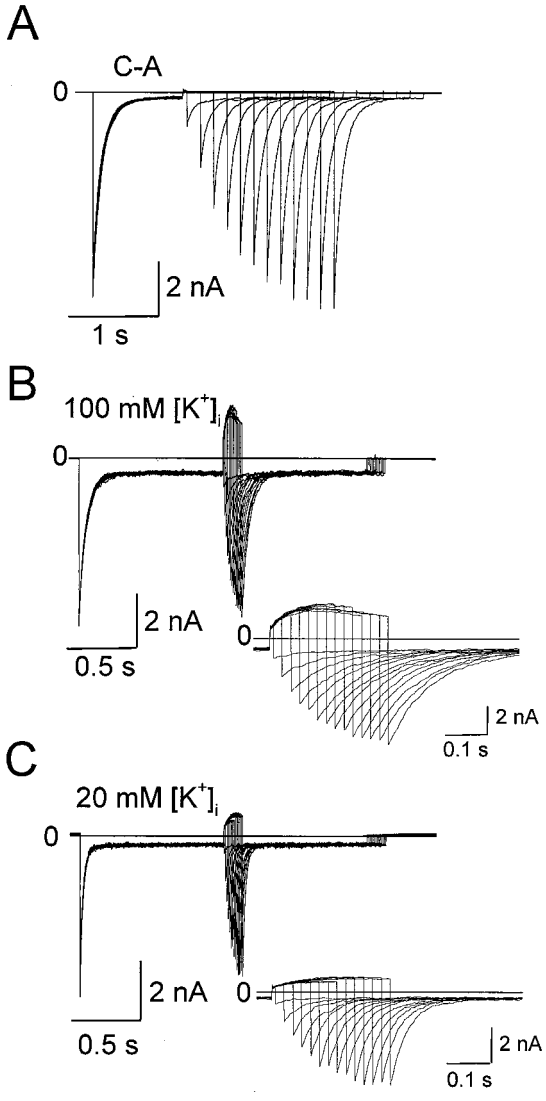

FIGURE 4 Effects of $[K^+]_i$ on the time course of recovery from extracellular Ba^{2+} blockade of the inward $I_{Kir2.1}$. (*A*) Current traces were recorded at $V_m = -120$ mV from a holding potential of 0 mV and $V_r = +100$ mV in a cell-attached patch. (*B* and *C*) Currents were recorded from the same patch shown in *A* after excising into the Mg^{2+}- and polyamine-free solution containing 100 mM $[K^+]_i$ and 20 mM $[K^+]_i$, respectively. The blockade of $I_{Kir2.1}$ was induced by the presence of 10 μM $[Ba^{2+}]$ in the pipette solution. The insets in *B* and *C* display currents recorded during the second pulse in amplified time scales. The horizontal lines indicate the zero current level. The frequencies of stimulation were 0.067 Hz. The sampling rates were 1 kHz (*A*) and 2.5 kHz (*B* and *C*).

blocker. We can distinguish between these two possibilities by examining the effects of $[K^+]_i$ on the kinetics of extracellular Ba^{2+} blockade. If K^+ competes with Ba^{2+} for a binding site, then k_{on} should be affected but k_{off} should not be affected by $[K^+]_i$. On the other hand, if K^+ knocks off Ba^{2+}, k_{off} should be affected.

Table 1 summarizes the effects of various $[K^+]_i$ on the extracellular Ba^{2+} blockade of the Kir2.1 channels with $V_r = +100$ mV. τ_{recov} was about one order of magnitude faster in the inside-out excised patches perfused with the control intracellular solution compared to cell-attached patches. Furthermore, τ_{block} was smaller in the inside-out patches than in the cell-attached patches. When $[K^+]_i$ was increased from 20 to 200 mM, τ_{recov} decreased, whereas τ_{block} increased. In addition, the fractions of nonblocked channels at the end of the -120-mV pulse increased as intracellular [K] increased. These results indicate that K^+ ions interfere with extracellular Ba^{2+} blockade of the Kir2.1 channels at $V_m = -120$ mV. To examine how $[K^+]_i$ affects the kinetic parameters for the extracellular Ba^{2+} blockade of $I_{Kir2.1}$ recorded at -120 mV, we estimated k_{on} and k_{off} using Eqs. 3 and 4, respectively. Note that here $f = I_{ss,Ba}/I_{inst,Ba}$; $I_{ss,Ba}$ and $I_{inst,Ba}$ are the steady-state and instantaneous currents recorded at -120 mV in the presence of 10 μM $[Ba^{2+}]_o$. The accurate expression of f should be $I_{ss,Ba}/I_{ss,ctrl}$, where $I_{ss,ctrl}$ is the steady-state current recorded at -120 mV in the absence of extracellular Ba^{2+}. Because currents were recorded in inside-out patches, we were not able to obtain both $I_{ss,Ba}$ and $I_{ss,ctrl}$ in the same patch. However, we consistently observed that the inward currents recorded in inside-out patches perfused with Mg^{2+}-free and polyamine-free solution did not decrease over time when there was no Ba^{2+} in the pipette (Fig. 6, *A* and *B*), and that 10 μM $[Ba^{2+}]_o$ only inhibited 5 $\pm$ 2% of the instantaneous inward $I_{Kir2.1}$ in whole-cell experiments. These observations support our assumption that $I_{inst,Ba} \approx I_{ss,ctrl}$. The averaged k_{on} and k_{off} values at different $[K]_i$ are summarized in Table 1. The results show that increasing $[K^+]_i$ decreased k_{on} without significantly affecting k_{off} for the binding of Ba^{2+} to the channels at -120 mV. Thus intracellular K^+ appears to relieve Ba^{2+} blockade by competing for the Ba^{2+} binding site in the channel.

Spermine contributes to the slow recovery from extracellular Ba^{2+} blockade in cell-attached patches

Fig. 4 demonstrates that the rates of recovery from Ba^{2+}-induced blockade were faster in inside-out patches exposed to Mg^{2+}-free and polyamine-free control solution containing 100 mM $[K]_i$ than those observed in cell-attached patches. To examine whether intracellular Mg^{2+} and spermine were responsible for the difference between the recovery rates obtained in the whole cells (or cell-attached patches) and the inside-out patches, we examined the effects of perfusing patches with the control intracellular solution containing Mg^{2+} or spermine on the recovery from the extracellular Ba^{2+} blockade. Fig. 5 *A* shows a set of current traces recorded from an inside-out patch exposed to the control intracellular solution, using the two-pulse voltage protocol. Perfusing this patch with the control intracellular solution containing 1 mM free $[Mg^{2+}]$ induced a slight increase in the recovery time constant from the control value of 45 ms (Fig. 5 *A*) to 99 ms (Fig. 5 *B*). Note that outward $I_{Kir2.1}$ at $V_r = +100$ mV was blocked. However, when the same patch was exposed to the control solution containing 100 μM spermine, the block time constant was

TABLE 1 Effects of various intracellular cations on the kinetics of the extracellular Ba^{2+} blockade of $K_{ir2.1}$ channels

	C-A ($n = 8$)	100 mM $[K^+]_i$ ($n = 14$)	200 mM $[K^+]_i$ ($n = 4$)	20 mM $[K^+]_i$ ($n = 3$)	+1 mM $[Mg^{2+}]_i$ ($n = 4$)	+100 μM $[spm]_i$ ($n = 3$)
τ_{block} (ms)	104.3 ± 10.4§	53.3 ± 2.3	65.0 ± 7.7*	24.0 ± 1.5#	70.8 ± 0.8#	122.7 ± 5.9#
τ_{recov} (ms)	412.3 ± 33.6§	38.1 ± 1.9	32.3 ± 3.4*	57.1 ± 6.0*	82.8 ± 5.9#	2300 ± 503§
f	0.05 ± 0.00§	0.12 ± 0.01	0.20 ± 0.03*	0.08 ± 0.01*	0.07 ± 0.01#	0.05 ± 0.03#
k_{on} ($10^6 \times s^{-1}M^{-1}$)	1.00 ± 0.15§	1.71 ± 0.12	1.31 ± 0.23*	3.85 ± 0.25*	ND	ND
k_{off} (s^{-1})	0.54 ± 0.11§	2.31 ± 0.11	3.17 ± 0.47 ($p = 0.24$)	3.49 ± 0.65 ($p = 0.17$)	ND	ND

Paired t-tests were carried out by comparing data in various groups to the control 100 mM K_i solution group.
*,#,§The groups were statistically different at $p < 0.05$, $p < 0.005$, and $p < 0.0005$, respectively, unless otherwise indicated.
+1 mM $[Mg^{2+}]_i$ = control 100 mM $[K^+]_i$ solution containing 1 mM free $[Mg^{2+}]$; +100 μM $[spm]_i$ = control solution containing 100 μM spermine.
τ_{recov} was obtained from $I_{Kir2.1}$ recorded with $V_r = +100$ mV at $V_m = -120$ mV; τ_{block}, f, k_{on}, and k_{off} were obtained at $V_m = -120$ mV.
ND, not determined.

increased, the recovery time course was dramatically retarded (Fig. 5 *C*, $\tau_{recov} = 3071$ ms), and the outward $I_{Kir2.1}$ was completely blocked. The effects of 1 mM free $[Mg^{2+}]_i$ and 100 μM spermine on the extracellular Ba^{2+} blockade of the Kir2.1 channels are also summarized in Table 1. These results suggest that spermine, but not Mg^{2+}, is one of the major factors that contribute to the slow recovery from extracellular Ba^{2+} blockade observed in whole cells and cell-attached patches, possibly by prohibiting the interaction between the bound Ba^{2+} and K^+. Becauase intracellular Mg^{2+} and spermine inactivated the inward $I_{Kir2.1}$ recorded in the absence of extracellular Ba^{2+} (data not shown), k_{on} and k_{off} were not determined in patches treated with Mg^{2+} or spermine.

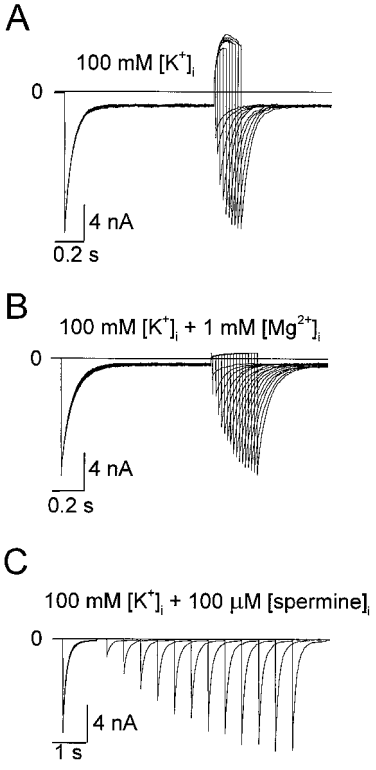

FIGURE 5 Effects of intracellular Mg^{2+} and spermine on the recovery of the inward $I_{Kir2.1}$ from blockade by extracellular Ba^{2+}. *A*, *B*, and *C* are the current traces recorded in an inside-out patch perfused with the control solution, the control solution containing 1 mM free $[Mg^{2+}]$, and the control solution containing 100 μM spermine, respectively. The same voltage protocol as described in Fig. 4 was applied. The frequencies of stimulation were 0.067 Hz in *A* and *B* and 0.04 Hz in *C*. Sampling rates were 2.5 kHz (*A* and *B*) and 0.5 kHz (*C*).

Blockade of Kir2.1 channels by intracellular Ba^{2+}

To examine whether Kir2.1 channels are inhibited by intracellular Ba^{2+}, we recorded $I_{Kir2.1}$ from excised inside-out giant patches. The $I_{Kir2.1}$ at positive and negative voltages were recorded in the absence of intracellular Mg^{2+} and polyamines. Fig. 6 shows the effects of 0, 0.1, and 3 μM $[Ba^{2+}]_i$ on the $I_{Kir2.1}$ recorded at +50 and −50 mV (Fig. 6 *A*) and at +30 and −30 mV (Fig. 6 *B*) from a holding potential of 0 mV and a prepulse voltage = −40 mV. As previously described (Shieh et al., 1996), control $I_{Kir2.1}$ ($[Ba^{2+}]_i = 0$) at +50 mV showed inactivation. In contrast, the current recorded at −50 mV was nearly constant throughout the 1.2-s period. The perfusion of the intracellular side of the membrane with 0.1 and 3 μM $[Ba^{2+}]$ resulted in reductions of the currents at the end of depolarization to +50 or +30 mV and acceleration of the inactivation of the outward $I_{Kir2.1}$. In contrast to the effects on outward $I_{Kir2.1}$, 0.1 and 3 μM $[Ba^{2+}]_i$ caused no change in the inward $I_{Kir2.1}$ recorded at −50 or −30 mV. All of these effects were reversible upon Ba^{2+} removal.

The normalized current-voltage relationships in the presence of 0, 0.1, and 3 μM $[Ba^{2+}]$ are shown in Fig. 6 *C*. The normalized $I_{Kir2.1}$ under control condition showed inward rectification at positive potentials, reflecting the presence of intrinsic inactivation. Intracellular Ba^{2+} induced a dose-dependent and V_m-dependent inhibition of the outward currents.

Fig. 7 *A* displays from right to left the dose-response curves for the $I_{Kir2.1}$ blockade by intracellular Ba^{2+} at +10, +20, +30, +40, +60, and +80 mV. The currents recorded at the end of the 1.2-s pulses in the presence of intracellular Ba^{2+} were normalized to the control at each voltage and expressed as fractional $I_{Kir2.1}$. Relations of the fractional $I_{Kir2.1}$ versus $[Ba^{2+}]_i$ were fitted by the Hill equation (Eq. 1). Fig. 7 *B* shows that K_d obtained from fitting in Fig. 7 *A*

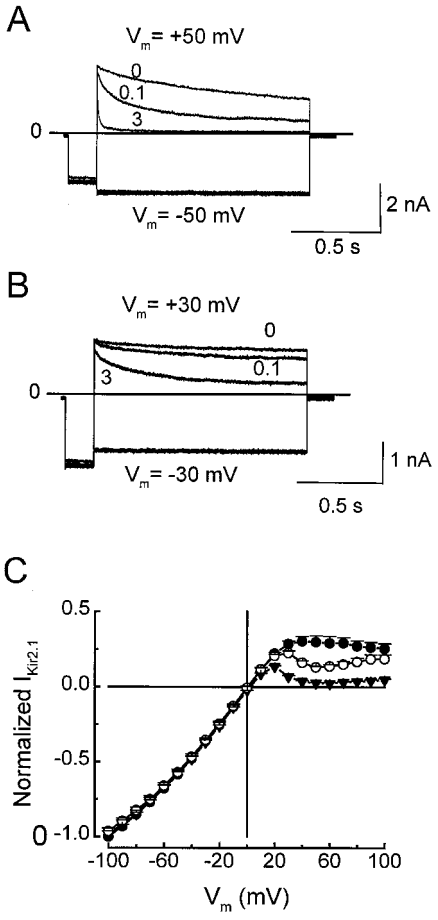

FIGURE 6 Blockade of Kir2.1 channels by intracellular Ba^{2+}. $I_{Kir2.1}$ was recorded at +50 and −50 mV (*A*) and at +30 and −30 mV (*B*) in the presence of 0, 0.1, and 3 μM $[Ba^{2+}]_i$. The residual current obtained in the presence of 30 mM intracellular TEA was used to subtract leak and capacitative components. The horizontal lines indicate the zero current level. (*C*) Normalized *I-V* relationships in the presence of 0 (control, ●, $n = 5$), 0.1 (○, $n = 5$), and 3 μM $[Ba^{2+}]_i$ (▼, $n = 5$). $I_{Kir2.1}$ measured at the end of the pulse was normalized to the values obtained at −100 mV in the absence of Ba^{2+}. The frequency of stimulation was 0.15 Hz, and the sampling rate was 5 kHz.

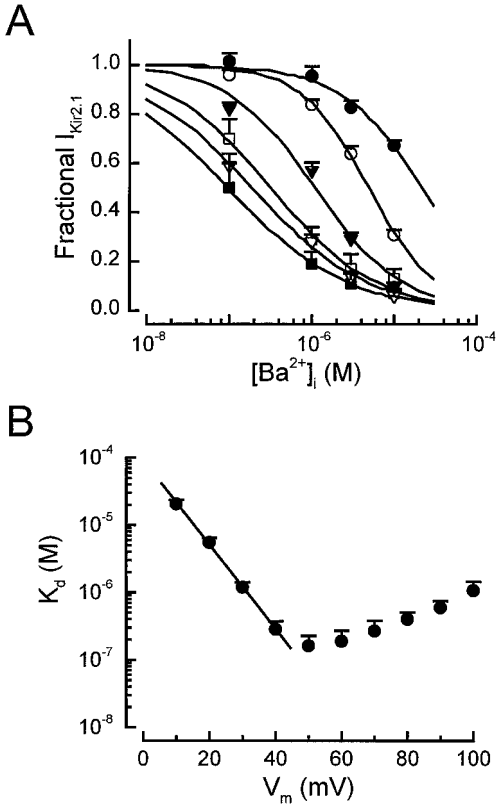

FIGURE 7 Dose-response curves and voltage dependence of Kir2.1 channel blockade by intracellular Ba^{2+}. (*A*) Dose-response curves at +10 (●), +20 (○), +30 (▼), +40 (▽), +60 (■), and +80 (□) mV were constructed for intracellular Ba^{2+} blockade of steady state $I_{Kir2.1}$. Data were fitted with the Hill equation (Eq. 1, *continuous lines*). The fit K_d and n values were 0.32 μM, 0.69, V_m = +80 mV; 0.10 μM, 0.61, V_m = +60 mV; 0.19 μM, 0.63, V_m = +40 mV; 1.09 μM, 0.83, V_m = +30 mV; 4.91 μM, 1.07, V_m +20 mV; 22.00 μM, 0.87, V_m +10 mV. (*B*) Voltage-dependence of K_d. K_d at V_m between +10 and +40 mV were fitted (*continuous line*) with the Boltzmann equation (Eq. 2) with K_d (0) = 91 μM and $z\delta = 3.57$.

was steeply dependent on V_m between +10 and +40 mV, and the K_d-V_m relationship fit well with the Boltzmann equation (Eq. 2). The $K_d(0)$ was 91 μM, and the δ value was 1.79, indicative of the multiionic pore feature of the Kir2.1 channel (Armstrong et al., 1982; Cecchi et al., 1987). In contrast, K_d showed a slight tendency to increase at $V_m \geq$ +40 mV.

It was previously shown that the inactivation of outward Kir2.1 currents recorded at $V_m \geq$ +40 mV followed a double-exponential time course and that this inactivation may be due to a pH_i-sensitive intrinsic gating movement (Shieh et al., 1996). To analyze the effects of intracellular Ba^{2+} on the two time constants that describe the inactivation of the outward $I_{Kir2.1}$, currents recorded at $V_m \geq$ +40 mV were fitted with a double-exponential function, and the time constants were extracted at each potential and $[Ba^{2+}]_i$. The time constants τ_1 (fast, Fig. 8 *A*) and τ_2 (slow, Fig. 8 *B*) calculated from currents recorded in various Ba^{2+} were normalized to the time constants calculated in the absence of Ba^{2+} and are shown as a function of membrane potential. Both τ_1 and τ_2 were decreased by intracellular Ba^{2+} in a dose-dependent but voltage-independent manner. These results suggest that once intracellular Ba^{2+} was bound to the channel, it interfered with the intrinsic gating process of the channel in a manner that accelerated the inactivation process.

DISCUSSION

Blockade of Kir2.1 channels by extracellular Ba^{2+}

The blockade of inward rectifier K^+ channels by extracellular Ba^{2+} has been extensively studied in starfish eggs (Hagiwara et al., 1978) and in frog skeletal muscle fibers (Standen and Stanfield, 1978). These studies showed that extracellular Ba^{2+} blocked the inward currents in a V_m- and time-dependent manner. The $K_d(0)$ values for Ba^{2+} blockade of the inward rectifier K^+ channels in starfish egg and

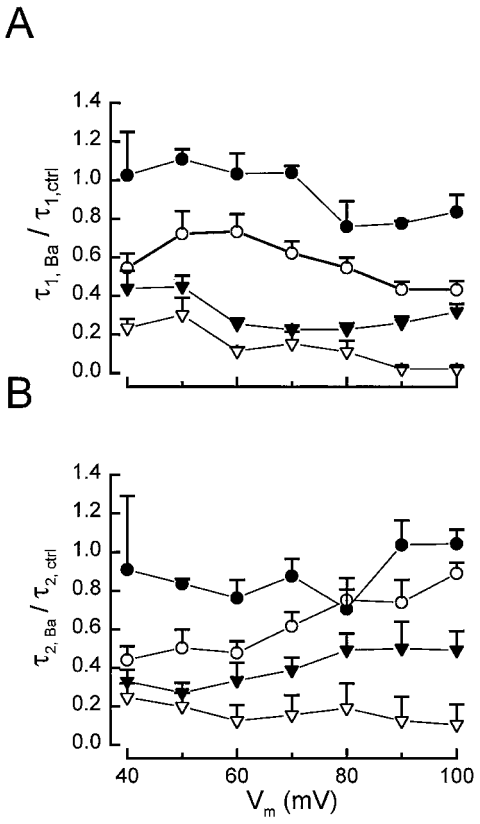

FIGURE 8 Acceleration of outward $I_{Kir2.1}$ inactivation by intracellular Ba^{2+}. The $\tau_{1,Ba}/\tau_{1,Ctrl}$-$V_m$ relationship (*A*) and $\tau_{2,Ba}/\tau_{2,Ctrl}$-$V_m$ relationship (*B*) for 0.03 (●, $n = 3$), 0.1 (○, $n = 11$), 1.0 (▼, $n = 11$), and 10 (▽, $n = 8$) μM $[Ba^{2+}]_i$.

frog skeletal muscle were 560 and 500 μM, respectively (Hagiwara et al., 1978; Standen and Stanfield, 1978). The effects of extracellular Ba^{2+} on these tissues were interpreted as the binding of Ba^{2+} to sites located within the pores of the channels where they sensed 64–70% of the electrical field (Hagiwara et al., 1978; Standen and Stanfield, 1978). The $K_d(0)$ value obtained for the extracellular Ba^{2+} blockage of the Kir2.1 channels was 62 μM, suggesting that cloned Kir2.1 channels are about one order of magnitude more sensitive to extracellular Ba^{2+} than the native inward rectifier K^+ channels in starfish egg or in frog skeletal muscle. Furthermore, the apparent electrical distance ($\delta = 0.54$) in Kir2.1 channels was smaller in the oocyte expressed channels than in the native channels.

Our results demonstrated that extracellular Ba^{2+} entered the pores to induce blockade of Kir2.1 channels as previously described in cloned and native inward rectifier K^+ channels. In addition, we showed that the K_d-V_m relationship became less steep as $V_m < -120$ mV, and k_{off} values increased when $V_m < -130$ mV. These observations are similar to those reported in the high-conductance Ca^{2+}-activated K^+ channels (Neyton and Miller, 1988b) and Skaker K^+ channels (Harris et al., 1998) and suggest that extracellularly applied Ba^{2+} can dissociate into the intracellular space at very hyperpolarizing potentials. On the other hand, k_{off} estimated from recovery of Ba^{2+} blockade increased as V_m became more positive. This suggests that the majority of Ba^{2+} dissociated into the extracellular space in a V_m-dependent manner.

Interactions of intracellular cations with Ba^{2+} applied extracellularly

Consistent with the previous finding that permeant K^+ can compete with Ba^{2+} for binding within the pores of the Ca^{2+}-activated K^+ channels (Vergara and Latorre, 1983), we demonstrated that in Kir2.1 channels, increasing $[K^+]_i$ from 20 to 200 mM increased the rate of recovery from extracellular Ba^{2+} blockade by decreasing the Ba^{2+} entrance rate (Fig. 3 *C* and Table 1). We also found that when an inside-out patch was perfused with Mg^{2+}-free and polyamine-free control solution, the recovery from extracellular Ba^{2+} (10 μM) blockade was much faster than in whole cells or cell-attached patches. One of the intracellular factors that contributed to the slow recovery from extracellular Ba^{2+} blockade in cell-attached patches was identified as spermine. We found that although spermine carries a +4 charge, it was not as efficient as intracellular K^+ or Mg^{2+} in facilitating the dissociation of the bound Ba^{2+} from the pore of a Kir2.1 channel at $V_r = +100$ mV. Note that in the presence of extracellular Ba^{2+}, spermine (100 μM) was still able to completely block the outward $I_{Kir2.1}$ at $V_r = +100$ mV, which indicates that spermine bound to its binding site(s) in the pore of the channel. These results provide evidence that a spermine binding site(s) is distinct from that for K^+ or Mg^{2+}.

In summary, the interactions of extracellular applied Ba^{2+} with other cations in the pore of the Kir2.1 channel are very complicated. So far we have identified a common binding site for K^+ and Ba^{2+} and a distinct site for spermine in the Kir2.1 channel. Further investigation is required to determine whether Kir2.1 channels have Ba^{2+} lock-in and enhancement sites lined up with the Ba^{2+} binding site similar to those described in the high-conductance Ca^{2+}-activated K^+ channels (Neyton and Miller, 1988b).

Blockade of Kir2.1 channels by intracellular Ba^{2+}

Intracellular Ba^{2+} at submicromolar concentrations blocked and accelerated the rate of inactivation of the outward $I_{Kir2.1}$. $[Ba^{2+}]_i$ higher than 10 μM resulted in complete inhibition of outward currents with very little blockade of the inward currents activated by hyperpolarization. All of these effects were observed in the absence of intracellular Mg^{2+} and polyamines. Fig. 7 *B* shows that K_d values for the inhibition of the outward currents decreased sharply as the depolarization increased until a minimum value of 0.16 ± 0.07 μM was reached at +50 mV. As depolarization became more positive, K_d for intracellular Ba^{2+} blockade of the outward $I_{Kir2.1}$ increased. This may be due to the dissociation of Ba^{2+} into the extracellular space facilitated by

depolarization, as previously shown for Na^+ permeating through the K^+ channels of the squid giant axon (French and Wells, 1977). Alternatively, this may be a result of the limitation of Ba^{2+} access to its binding site when the intrinsic inactivation gate closed the channel. Our experimental data also demonstrate that the exposure of the intracellular side of the channels to Ba^{2+} results in an acceleration of the inactivation at positive voltages. It is tempting to propose that Ba^{2+} may directly interact with the intrinsic gating mechanism responsible for the inactivation of Kir2.1 channels at positive voltages. The possibility of Ba^{2+} interaction with the intrinsic gate renders it a useful tool for probing the movement of the intrinsic gate of the Kir2.1 channels.

In conclusion, in this study we report the voltage-dependent blocking effects of both intracellular and extracellular Ba^{2+} on the cloned inward rectifier K^+ channel Kir2.1. Ba^{2+} applied extracellularly can enter the pore of a Kir2.1 channel and dissociate into the intracellular space at very negative membrane potentials. Our study of the effects of intracellular cations on the recovery from Ba^{2+} blockade suggest that various cations entering the pore of a Kir2.1 channel may occupy different binding sites. Whereas Mg^{2+} produced a degree of efficiency similar to that of K^+ in relieving Ba^{2+} blockade, spermine bound in the channel was much less effective in enhancing the dissociation of Ba^{2+} from the pore. We also showed that intracellular Ba^{2+} closely interacts with the "intrinsic" gate and may be applied to reveal the characteristics of this "intrinsic" gating mechanism in Kir2.1 channels.

We thank Dr. Patricia Pérez (UASLP, Mexico) and Dr. Jim Weiss (UCLA, USA) for their critical reading of the manuscript and helpful comments on this study and Mr. Douglas Platt for editing the English of the manuscript.

This work was supported by National Science Council grant 86-2314-B-001-025; Academia Sinica, Taiwan, R.O.C.; and the Fundación Mexicana para la Salud and Fondo de Apoyo a la Investigación, UASLP, Mexico.

REFERENCES

Armstrong, C. M., R. P. Swenson, and S. R. Taylor. 1982. Block of squid axon K channels by intracellularly and extracellularly applied barium ions. *J. Gen. Physiol.* 80:663–682.

Armstrong, C. M., and S. R. Taylor. 1980. Interaction of barium ions with potassium channels in squid giant axons. *Biophys. J.* 30:473–488.

Ashen, M. D., B. O'Rourke, K. A. Kluge, D. C. Johns, and G. F. Tomaselli. 1995. Inward rectifier K^+ channel from human heart and brain: cloning and stable expression in a human cell line. *Am. J. Physiol.* 268: H506–H511.

Cecchi, X., D. Wolff, O. Alvarez, and R. Latorre. 1987. Mechanism of Cs^+ blockade in a Ca^{2+}-activated K^+ channel from smooth muscle. *Biophys. J.* 52:707–716.

Eaton, D. C., and M. S. Brodwick. 1980. Effects of barium on the potassium conductance of squid axon. *J. Gen. Physiol.* 75:727–750.

Fickler, E., M. Taglialatela, B. Wible, C. Henley, and A. Brown. 1994. Spermine and spermidine as gating molecules for inward rectifier K^+ channels. *Science.* 266:1068–1071.

French, R. J., and J. B. Wells. 1977. Sodium ions as blocking agents and charge carriers in the potassium channel of the squid giant axon. *J. Gen. Physiol.* 70:707–724.

Hagiwara, S., S. Miyazaki, W. Moody, and J. Patlak. 1978. Blocking effects of barium and hydrogen ions on the potassium current during anomalous rectification in the starfish egg. *J. Physiol. (Lond.).* 279: 167–185.

Harris, R. E., H. P. Larsson, and E. Y. Isacoff. 1998. A permeant ion binding site located between two gates of the Shaker K^+ channel. *Biophys. J.* 74:1808–1820.

Hilgemann, D. W. 1995. The giant membrane patch. *In* Single-Channel Recording. B. Sakmann and E. Neher, editors. Plenum Press, New York. 307–328.

Hille, B. 1992. Potassium channels and chloride channels. *In* Ionic Channels of Excitable Membranes. Sinauer, Sunderland, MA. 115–139.

Hille, B., and W. Schwarz. 1978. Potassium channels as multi-ion single-file pores. *J. Gen. Physiol.* 72:409–442.

Holmgren, M., P. L. Smith, and G. Yellen. 1997. Trapping of organic blockers by closing of voltage-dependent K^+ channels. Evidence for trap door mechanism of activation gating. *J. Gen. Physiol.* 109:527–535.

Huang, C.-L., S. Feng, and D. W. Hilgemann. 1998. Direct activation of inward rectifier potassium channels by PIP_2 and its stabilization by $G_{\beta\gamma}$. *Nature.* 391:803–806.

Kubo, Y., T. Baldwin, Y. Jan, and L. Jan. 1993. Primary structure and functional expression of a mouse inward rectifier potassium channel. *Nature.* 362:127–133.

Lopatin, A., E. Makhina, and C. Nicols. 1994. Potassium channel block by cytoplasmic polyamines as the mechanism of intrinsic rectification. *Nature.* 372:366–371.

Makhina, E. N., A. J. Kelly, A. N. Lopatin, R. W. Mercer, and C. Nichols. 1994. Cloning and expression of a novel human brain inward rectifier potassium channel. *J. Biol. Chem.* 269:20468–20474.

Martell, A. E., and R. M. Smith. 1974. Critical Stability Constants. Plenum Press, New York.

Matsuda, H., A. Saigusa, and H. Irisawa. 1987. Ohmic conductance through the inwardly rectifying K^+ channel and blocking by internal Mg^{2+}. *Nature.* 325:156–159.

Morishige, K. I., N. Takahashi, A. Jahangir, M. Yamada, H. Koyama, J. S. Zanelli, and Y. Kurachi. 1994. Molecular cloning and functional expression of a novel brain-specific inward rectifier potassium channel. *FEBS Lett.* 346:251–256.

Neyton, J., and C. Miller. 1988a. Potassium blocks barium permeation through a calcium-activated potassium channel. *J. Gen. Physiol.* 92: 549–567.

Neyton, J., and C. Miller. 1988b. Discrete Ba^{2+} block as a probe of ion occupancy and pore structure in the high-conductance Ca^{2+}-activated K^+ channel. *J. Gen. Physiol.* 92:569–586.

Perier, F., C. M. Radeke, and C. A. Vandenberg. 1994. Primary structure and characterization of a small-conductance inwardly rectifying potassium channel from human hippocampus. *Proc. Natl. Acad. Sci. USA.* 91:6240–6244.

Shieh, R.-C., J.-C. Chang, and J. Arreola. 1998. Ba^{2+} blockade of the cloned inward rectifier K^+ channels Kir2.1 (IRK1) expressed in *Xenopus* oocytes. *Biophys J.* 74:A114.

Shieh, R.-C., S. A. John, J.-K. Lee, and J. N. Weiss. 1996. Inward rectification of the IRK1 channel expressed in *Xenopus* oocytes: effects of intracellular pH reveal an intrinsic gating mechanism. *J. Physiol. (Lond.).* 494:363–376.

Standen, N. B., and P. R. Stanfield. 1978. A potential- and time-dependent blockade of inward rectification in frog skeletal muscle fibres by barium and strontium ions. *J. Physiol. (Lond.).* 280:169–191.

Vandenberg, C. 1987. Inward rectification of a potassium channel in cardiac ventricular cells depends on internal magnesium ions. *Proc. Natl. Acad. Sci. USA.* 84:2560–2564.

Vergara, C., and R. Latorre. 1983. Kinetics of Ca^{2+}-activated K^+ channels from rabbit muscle incorporated into planar bilayers. *J. Gen. Physiol.* 82:543–568.

Yellen, G. 1984. Relief of Na^+ block of Ca^{2+}-activated K^+ channels by external cations. *J. Gen. Physiol.* 84:187–199.

Zhou, H., S. Chepilko, W. Schutt, H. Choe, L. Palmer, and H. Sackin. 1996. Mutations in the pore region of ROMK1 enhance Ba block. *Am. J. Physiol.* 271:C1949–C1956.